REPORT DOCUMENTATION PAGE

Form Approved
OMB No. 0704-0188

PLEASE DO NOT RETURN YOUR FORM TO THE ABOVE ADDRESS.

1. REPORT DATE *(DD-MM-YYYY)*	2. REPORT TYPE	3. DATES COVERED *(From - To)*
27-06-2007	Final Technical Report	September 1, 2006 - May 31, 2007

4. TITLE AND SUBTITLE

Fabrication of a lateral polarity GaN MESFET: an exploratory study

5a. CONTRACT NUMBER

W911NF-06-1-0406

5b. GRANT NUMBER

5c. PROGRAM ELEMENT NUMBER

6. AUTHOR(S)

Zlatko Sitar and Ramon Collazo

5d. PROJECT NUMBER

5e. TASK NUMBER

5f. WORK UNIT NUMBER

7. PERFORMING ORGANIZATION NAME(S) AND ADDRESS(ES)

North Carolina State University
Materials Science and Engineering
Campus Box 7919
Raleigh, NC 27695-7919

8. PERFORMING ORGANIZATION REPORT NUMBER

9. SPONSORING/MONITORING AGENCY NAME(S) AND ADDRESS(ES)

Army Research Office
ATTN: AMSRD-ARL-RO-SG-SI (Technical Reports)
P. O. Box 12211
Research Triangle Park, NC 27709-2211

10. SPONSOR/MONITOR'S ACRONYM(S)

ARO

11. SPONSOR/MONITOR'S REPORT NUMBER(S)

51926.1-EL-II

12. DISTRIBUTION/AVAILABILITY STATEMENT

Approved for public release; distribution unlimited.

13. SUPPLEMENTARY NOTES

14. ABSTRACT

This report describes exploratory studies in the fabrication of the GaN LPH structures and their application in the fabrication of a depletion-mode metal semiconductor field effect transistors (MESFETs). Exploiting LPH growth technology, and the difference in the electronic properties of the different type of domains, i.e. as grown N-polar domains are conductive and Ga-polar domains are insulating, laterally selective doped areas can be realized for improving contact resistance to the conduction channel in GaN MESFETs. Basically, the N-polar domains act as the ohmic contacts to the channel that is localized in a Ga-polar domain.

15. SUBJECT TERMS

GaN MESFET, lateral polar homojunction (LPH), MOVPE, polarity, doping selectivity

16. SECURITY CLASSIFICATION OF:			17. LIMITATION OF ABSTRACT	18. NUMBER OF PAGES	19a. NAME OF RESPONSIBLE PERSON
a. REPORT	b. ABSTRACT	c. THIS PAGE			Zlatko Sitar, Professor
Unclassified	Unclassified	Unclassified	Unlimited	15	19b. TELEPHONE NUMBER *(Include area code)* 919.515.8637

Reset

Fabrication of a lateral polarity GaN MESFET: an exploratory study

1. Introduction

The polarity control scheme for obtaining both Ga- and N-polar films on a sapphire substrate, allows the fabrication of GaN lateral polar homojunction (LPH) structures.[1] The possibility to control the GaN polarity was thought to be only possible by MBE.[2, 3] This ability provided innovative GaN based device applications.[4] However, the technical difficulties of using MBE as the growth technique have hindered the technological development of the III-nitrides family of devices. In contrast to the fabrication of LPH structures using MBE, LPH fabrication by MOVPE has lagged far behind, since numerous studies have been devoted to the realization of Ga-polarity and not N-polarity films.[5, 6] The growth of N-polar films by MOVPE was made possible by exposing a H_2-etched sapphire substrate to an ammonia atmosphere (nitridation) without an AlN nucleation layer (NL). The ability to control the polarity by MOVPE also makes the fabrication of a LPH structure possible. Therefore, progress is expected in GaN LPH structures by using the MOVPE process.

Selectivity of the GaN polarity grown by MOVPE in our process relies on presence or absence of low temperature (LT)-AlN on a sapphire substrate prior to the HT-GaN deposition. When GaN films are grown on a properly treated AlN NL, the resulting GaN films are Ga polar. On the other hand, when sapphire substrates are nitrided at high temperature (>950°C), the subsequent GaN layers are grown in the N-polar direction. Therefore, the appropriate template with a pattern of AlN/nitrided sapphire allows the simultaneous growth of both polar domains.

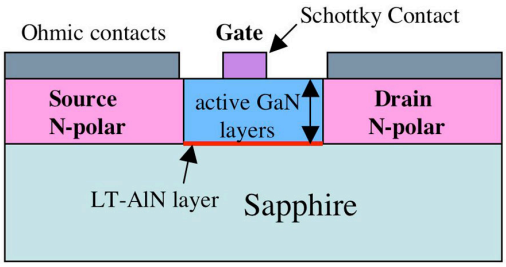

Figure 1. Basic structure of an LPH based GaN MESFET. The highly conductive N-polar domains are acting as source and drain regions. The active layers are within the Ga-polar domain.

This report describes exploratory studies in the fabrication of the GaN LPH structures and their application in the fabrication of a depletion-mode metal semiconductor field effect transistors (MESFETs). Exploiting LPH growth technology, and the difference in the electronic properties of the different type of domains, i.e. as grown N-polar domains are conductive and Ga-polar domains are insulating, laterally selective doped areas can be realized for improving contact resistance to the conduction channel in GaN MESFETs. Basically, the N-polar domains act as the ohmic contacts to the channel that is localized in a Ga-polar domain. Figure 1 shows the basic structure of an LPH based GaN MESFET in which the N-polar domains act as source and drain contacts to the channel.

2. *Fabrication Procedure*

The fabrication of a GaN LPH structure on a sapphire substrate requires three process steps: (1) deposition of a LT-AlN layer, (2) patterning of the AlN nucleation template, and (3) growth of the GaN layer. LT-AlN deposition and HT-GaN growth conditions have been described in detail elsewhere [reference]. Typically, both GaN polarities were grown simultaneously on patterned AlN templates following the growth conditions developed in the PIs' laboratories. N_2 was used as a carrier and diluent gas. HT-GaN growth conditions were kept constant with a V/III ratio of 100, an ammonia flow of 0.3 slm and a TEG flow of 36 μmol/min under a total flow rate of 7.5 slm. This growth conditions provided mass-transfer-limited growth with significant supersaturation.

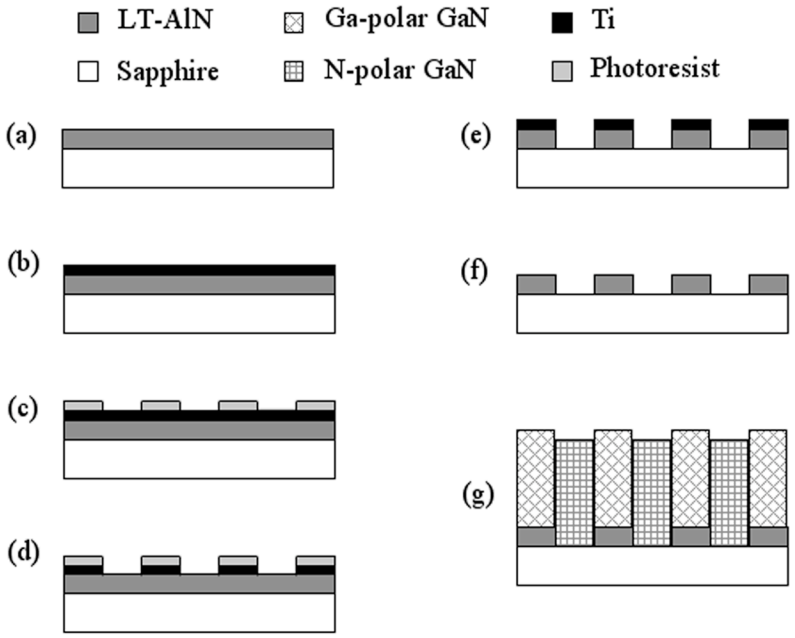

Figure 2. Developed process flow for fabrication of LPH GaN structures by MOCVD: (a) the growth of LT-AlN on sapphire, (b) deposition of Ti, (c) photoresist, (d) formation of stripe pattern by lithography, (d) KOH etch to expose the sapphire substrate, (e) removal of Ti, and (g) growth of GaN.

The process steps developed for the fabrication of GaN LPH structures are shown in Figure 2. Prior to deposition of the LT-AlN layer (Figure 2(a)), the (0001) sapphire substrate is exposed to a flow of H_2 at 1100°C for 7 min and then nitrided under a flow of NH_3 at 950°C for 4 min. The 10-20 nm thick LT-AlN NL is grown at 600°C and then annealed at a temperature of 1040°C under an ammonia partial pressure of 2 Torr (diluted in N_2) and a total gas molar flow rate of 2.2 slm. A typical anneal time of the AlN layer is 15 min. The sample is quenched to room temperature in order to carry out ex-situ lithography and patterning.

A thin Ti mask layer (~30 nm) is deposited on the sample (Figure 2(b)). Photoresist is then spun on the sample and patterned using optical lithography with the desired geometry (Figure 2(c)). Unmasked Ti regions are etched using a 0.1% HF to expose the

AlN layer (Figure 2(d)). After the removal of the photoresist mask by acetone, the unmasked AlN regions are etched down to the sapphire substrate using a hot (50°C) 6M KOH solution for 1 min (Figure 2(e)). The Ti mask is removed using 5 % HF. These lithography and etching procedures on the AlN layer result in a sample with AlN-coated and bare contiguous regions on sapphire (Figure 2(f)). The sample is cleaned using a de-ionized water rinse and dried with nitrogen before reintroduction into the MOVPE chamber.

After reintroduction of the sample into the MOVPE chamber, the temperature is ramped up for the GaN growth under an N_2 atmosphere. A nitridation step (2^{nd} nitridation) prior to the HT-GaN growth is necessary to obtain N-polar GaN on the exposed sapphire regions in the sample. The GaN growth is carried out at a temperature of 1040°C. Upon the completion of this step, the sample consists of a GaN LPH structure with Ga- and N-polarities (Figure 2(g)). Both polar domains are grown simultaneously at the same growth rate. Typical useful thickness is 1.5 µm and grown at a growth rate of 2 µm/hr. To realize the MESFET, after growth of this undoped GaN layer, a Si-doped (SiH_4 is used as source) n-type conducting channel is grown with the desired thickness and doping concentration. In this study, the channel thickness was chosen as 30 nm with a SiH_4 flow of 0.9 nmols/min. This SiH_4 dosage corresponded to a Si incorporation of 3-4x10^{18} cm^{-3}, as measured by Secondary Ion Mass Spectroscopy (SIMS). After a processing interrupt, a 30 nm cap of undoped GaN is grown on top of the channel. Since both types of domains were simultaneously grown, the source and drain contacts to the channel are already made at the end of the GaN growth, no subsequent step is needed. Figure 3 shows the region near the surface and the resulting final structure after metallization.

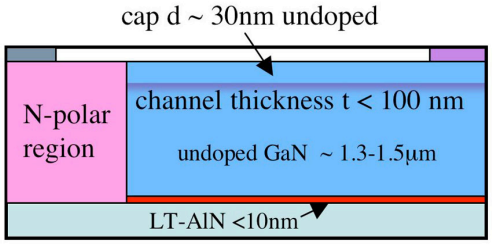

Figure 3. Region near the surface and the resulting structure after the deposition of the GaN layers. The N-polar regions form a lateral ohmic contact to the conducting channel.

The GaN LPH samples were studied by various characterization techniques. The surface morphology was observed by Differential Interference Contrast (DIC) optical microscopy and Scanning Electron Microscopy (SEM). Crystallographic characterization of the LPH sample was performed by acquiring on- and off-axis HRXRD ω-rocking curves using a Philips X'Pert Materials Research Diffractometer with a copper x-ray source and an open slit on the detector side in the double axis configuration. The geometry of the MESFET will depend on the application and specific capabilities for fabrication. Two geometries with different sizes can be fabricated: linear and circular. Circular MESFETs have the advantage of no need for trench isolation as the linear devices. This geometry was used to characterize the electrical operation of the MESFET. Ohmic contacts to the N-polar regions acting as source and drain were done by electron

beam (e-beam) evaporation of the following metal layer structure: 15 nm Ti/ 150 nm Al/ 80 nm Ni/ 80 nm Au. This structure is patterned and rapid thermal annealed (35 s at 850°C) to provide an excellent ohmic contact. The Schottky contact acting as the gate was realized by depositing via e-beam evaporation 100 nm Ni/100 nm Au and patterning for finalizing the gate structure. Figure 4 shows an optical microscope image of a circular (a) and a linear (b) MESFET after completing all the process steps. The smooth and rough regions are the Ga- and N-polar domains, respectively.

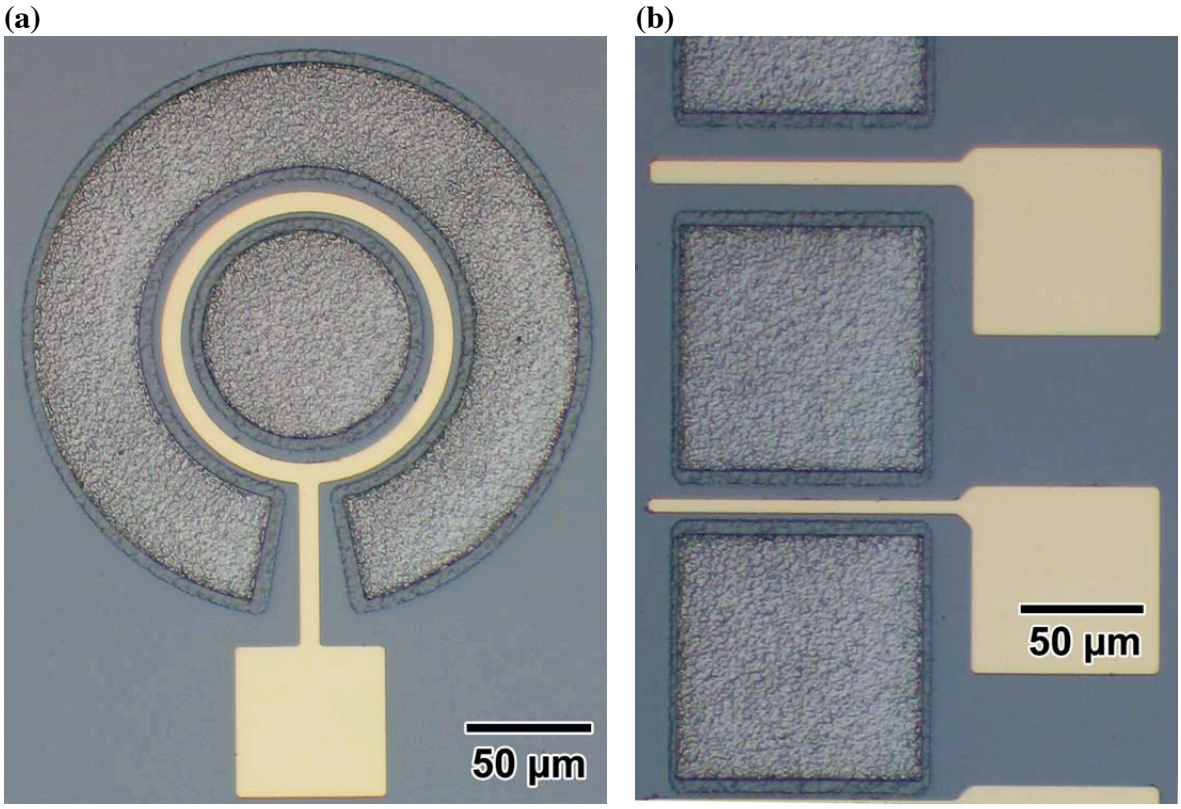

Figure 4. LPH circular(a) and linear (b) MESFET after completing all the process steps described in the text. Circular MESFETs were used to characterize the electrical operation of the device.

3. Demonstration of the GaN LPH structure

3.1. Fabrication conditions for the GaN LPH structure

Following the GaN polarity control scheme previously established, LT-AlN deposition on nitrided sapphire was carried out for 5.5 min and an anneal time of 15 min at 1040°C. After the fabrication of a patterned AlN template, the 2nd nitridation was carried out at 950°C for 1 minute. Following the 2nd nitridation, the growth of GaN was carried out at 1040°C. N-polar GaN was obtained on the exposed sapphire region of the template, while GaN grown on AlN region exhibited mixed-polarity. As previously discussed, N-polar GaN was consistently obtained on nitrided sapphire substrates

irrespective of nitridation conditions (temperature and time), while Ga-polar GaN required a proper LT-AlN thickness and anneal time. Additional *ex-situ* lithography and etching, processes necessary to fabricate patterned LT-AlN templates may alter the optimized Ga-polar GaN growth conditions from that of the conventional two-step growth process. Therefore, the necessary conditions for the LT-AlN thickness and annealing should be investigated in order to obtain pure Ga-polar domains on the intended regions of the LPH structure.

Although the use of KOH allowed determination of the polarity type of the GaN films, the chemical etching selectivity was sometimes hard to distinguish in samples that were mostly Ga-polar with a low density of inversion domains (ID). On the other hand, it was established that there were significant differences in the sheet resistance between Ga-polar and mixed-polar GaN films. Highly resistive Ga-polar GaN is advantageous in optoelectronic and electronic device applications, especially for MESFET operation. It reduces parallel conductivity and poor pinch-off characteristics originating from unintentional background carrier concentrations.

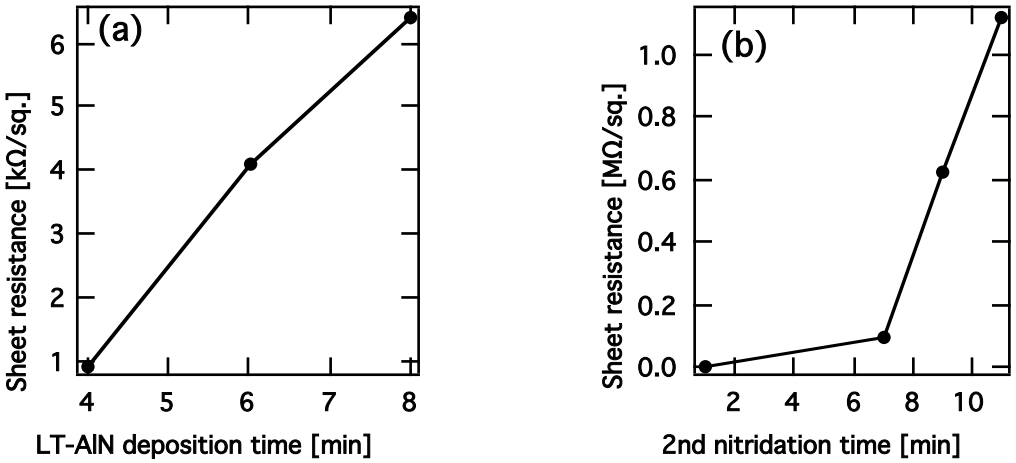

Figure 5. Sheet resistance of GaN grown on AlN region for the first set of LT-AlN layers deposited for 4, 6, and 8 min. 2nd nitridation time after ex-situ process was kept at 950°C for 1 min. (b) Sheet resistance of GaN grown on AlN region for the second set of 2nd nitridation time carried out at 1050°C for 1, 7, 9, and 11 min. LT-AlN deposition time was kept for 6 min.

Two sets of experiments were carried out to determine the conditions to achieve pure Ga-polar, highly resistive GaN on the AlN NL regions. The first set of experiments focused on the deposition time of the LT-AlN layer. After the *ex-situ* lithography and etching process, 2nd nitridation was kept constant with a temperature of 950°C for 1 minute. Figure 5(a) shows the sheet resistance of GaN grown on AlN regions that were deposited for 4, 6, and 8 minutes. Although GaN grown on AlN exhibited an increase in the sheet resistance with increasing deposition time, the sheet resistances still ranged from 1 kΩ/sq to 6 kΩ/sq indicating that in this case all Ga-polar domains were of mixed-polarity. These results contradict those obtained previously which showed that the LT-AlN deposition time strongly influences the sheet resistance as well as the polarity type. This suggests that a modification of the LT-AlN film occurred during the *ex-situ* process.

AlN is known to form oxides or hydroxides in the presence of water, making this a likely cause for the occurrence of IDs within the Ga-polar matrix.[7]

A second set of experiments was carried out with respect to the 2nd nitridation time. The AlN NL deposition time was kept constant at 6 min and the anneal temperature was 1050°C, higher than that used for the first set of experiments. 2nd nitridation time was varied from 1 min to 11 min. Figure 2(b) shows the sheet resistance of GaN as a function of the 2nd nitridation time. Compared to Figure 2(a), the overall sheet resistances were 3 orders of magnitude higher. This indicated that a higher temperature nitridation improved sheet resistance of GaN. Furthermore, the maximum sheet resistance was obtained in a nitridation that was 11 minutes long. This nitridation may have played a role in transforming the oxide or hydroxide that may have formed on the LT-AlN as well as helping in obtaining N-polar GaN on the exposed sapphire region.

3.2. Determination of polarity for the GaN LPH structure

Figure 6 shows a DIC optical micrograph (plane-view) (a) and SEM image (cross-section) of Ga- and N-polar layers grown side-by-side. Figure 6(a) shows that the Ga-polar domains exhibited smooth, featureless morphology, while the N-polar domains exhibited hexagonal facetted morphology. Figure 6(b) shows a cross-sectional SEM image in the vicinity of the IDB. The region left of the boundary was the Ga-polar domain, while the region right of the boundary was the N-polar domain. Cross-sectional SEM images revealed that no difference in thickness between the two domains was observed within 30 μm of each side of the boundary (Figure 6(b)). Micrographs taken farther away from the boundary, within each domain, did not show any difference in thickness. The identical growth rate was attributed to the GaN growth condition used, that is, a low V/III ratio under a N_2 atmosphere. These conditions provided a mass-transfer-limited growth regime with a large supersaturation. The process used N_2 as a carrier gas and dilution gas in contrast to the commonly used H_2.

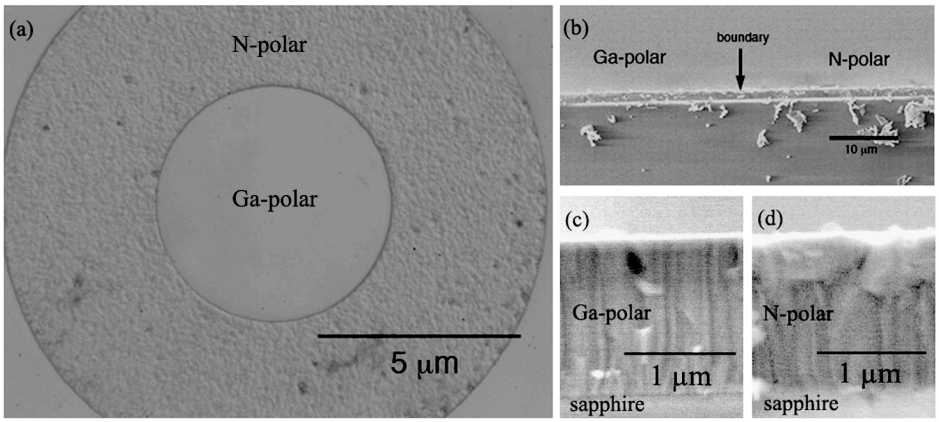

Figure 6. Plane view and cross-sectional image of the GaN LPH structure. (a) DIC image of plane-view of the LPH structure. (b) Cross-sectional SEM around the IDB. Cross-sectional SEM of the Ga-polar domain (c) and N-polar domain (d).

In addition, Transmission Electron Microscopy (TEM) was used to determine the polarity of the GaN LPH. Specifically, Convergent Beam Electron Diffraction (CBED)

was used for this purpose.[8] Two TEM samples made out of the LPH were prepared, a cut along the {-2110}and {-1100} planes. The former one was use to determine the atomic structure from Z-contrast imaging while the latter one was used to determine the polarity of GaN with CBED due to its more obvious features in the diffraction discs. The polarity of GaN was determined by CBED from two different positions across the interface. By comparing the diffraction patterns to the simulated CBED patterns, it was evident that the two different regions on either side of IDB exhibited opposite polarities. A transition region separating the Ga-polar and the N-polar domains was observed; it's width was typically around 100 nm and consisted of mixed-polar GaN, that is, a Ga-polar matrix with N-polar inversion domains. The occurrence of this mixed-polar transition region at the interface between the two domains is likely due to the poorly defined edge of the LT-AlN caused by the photolithography process or over-etching of the film (under the Ti mask). Otherwise, no overgrowth of any of the domains was observed, i.e. the intended position of the boundary was maintained (within processing limits).

4. Electrical and structural characterization of the LPH

Electrically insulating Ga-polar domains were achieved by optimization of the 2nd nitridation conditions. The electrical characteristics for both polar domains were investigated by Van der Pauw/Hall measurements. It was impossible to conduct Hall measurements on the Ga-polar domains; the unintentionally doped Ga-polar domains showed insulating behavior with a sheet resistance exceeding 1 MΩ/sq, the limit of the measurement setup. N-polar domains showed distinctly different electrical properties. It is interesting to note that the electrical characteristics of the N-polar domains were almost unchanged in spite of a significant change in the surface morphology, from a relatively smooth surface to hexagonal facets with the increase in nitridation time and temperature. The unintentionally doped N-polar domains were always highly n-type conductive, with a typical resistivity of 2.1 mΩcm. Hall measurements revealed an n-type carrier concentration of $3x10^{19}$ cm^{-3} for unintentionally doped material with a mobility of 100 cm^2/Vs. This mobility can rival state-of-the-art Ga-polar GaN material at this high doping concentrations.[9]

This n-type conductivity in N-polar GaN was consistent with observations from other authors.[10, 11] The origin for the n-type conductivity in this material was not clear; however, there is a high possibility that residual oxygen may be acting as a donor in GaN.[12] The probability of incorporating oxygen as a donor impurity into N-polar GaN is higher than the probability of incorporation into Ga-polar GaN.[11] Oxygen was found to be an impurity with up to three orders of magnitude higher concentration in N-polar domains than in the Ga-polar domains as measured by SIMS. The incorporation of oxygen in the two different domains did not depend on the growth process, but rather on the growth orientation. In addition, this conductivity is bulk conductivity and not merely an effect of mobile surface charge; N-polar layers with different thicknesses showed sheet conductivity that scaled with the layer thickness.

Figure 7 shows the full-width at half maximum (FWHM) of the (00.2), (10.3), (30.2) reflections as a function of the plane inclination angle with respect to the (00.2) direction for Ga-polar domains and N-polar domains from an LPH structure. Rocking curves were measured for each type of domain away from the boundary where the two domains meet. The (00.2) reflection was measured in a symmetric geometry, while the (10.3) and (30.2)

reflections were measured in a skew-symmetric geometry. The FWHM of the (00.2) symmetric reflection for a N-polar film is 700 arcsec, slightly higher than the FWHM of the same reflection for the Ga-polar, less than 400 arcsec. However, similar FWHM of the off-axis reflections were observed. It was revealed that the N-polar domains had a comparable structural quality to that of the Ga-polar domains, even thought there was a significant difference in the surface morphology.

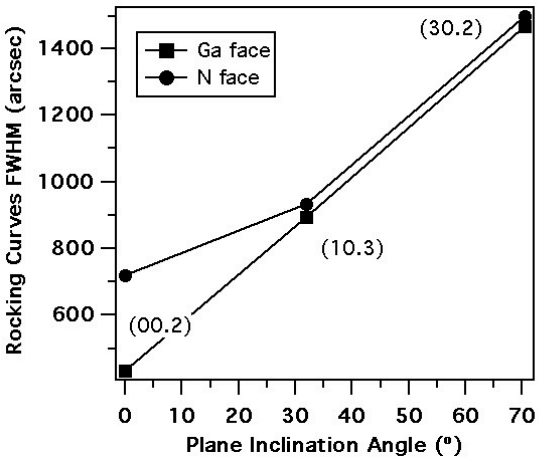

Figure 7. X-ray rocking curves FWHM of the (00.2), (10.3), (30.2) reflections as a function of the plane inclination angle with respect to the (00.2) on-axis reflection for Ga-polar domain and N-polar domain from the LPH structure. Rocking curves were measured for each type of domain away from the boundary.

The dislocation density with edge component was estimated to be 1×10^{10} cm^{-2} from the FWHM values of the (30.2) rocking curve.[13] Edge dislocations are known to act as acceptor-level traps, and thus may play a significant role in carrier compensation in the GaN films.[14] Nevertheless, the contrast in the electrical conductivity between the two different domains at almost the same dislocation density with edge component implies that carrier compensation alone does not account for the high resistivity of the Ga-polar domains, a significant decrease of the donor impurity due to the removal of inversion domains within the Ga-polar domain should account for the increase in resistivity. In N-polar domains, the high donor impurity incorporation such as oxygen is the cause for the high background carrier concentration and it is not entirely compensated by dislocations. Thus, reduction of IDs until dislocations or point defects compensate the related residual donors can be thought to be the mechanism for obtaining highly resistive Ga-polar domains. Still, this compensation effect is relatively small compared to the significant polarity dependent difference in impurity incorporation brought by IDs. This observation also follows from figure 5(b), where there was an increase in sheet resistance as a function of the 2nd nitridation. Since the dislocation density with the edge component as estimated from the (30.2) reflection remained the same, no increase in carrier compensation from the dislocations was possible. The FWHM value of the (30.2) reflection was ~1300 arcsec for all the films represented in Figure 5(b).

5. Electronic behavior of the inversion domain boundary (IDB)

In the last sections, it was demonstrated that Ga-polar and N-polar domains were simultaneously grown side-by-side following our process discussed above. It was revealed that both polar domains had significant differences in their characteristics. The electrical behavior of the interface between the two domains is of particular interest, especially with respect to possible applications of this GaN LPH structure to electronic and optoelectronic devices. In this study, it is of interest to use the LPH as laterally selective doped areas to be used as ohmic contacts to active current channels in FETs to decrease contact resistance. No electronic potential energy barrier for carriers across the inversion domain boundary (IDB) of the GaN LPH is desirable for this application. To investigate the existence of an electronic potential barrier, both Ga-polar and N-polar domains should be conductive. As previously mentioned, the sheet resistance of Ga-polar domains exceeded 1 MΩ/sq. The Ga-polar domains needed to be doped with Si for possible electrical measurements.

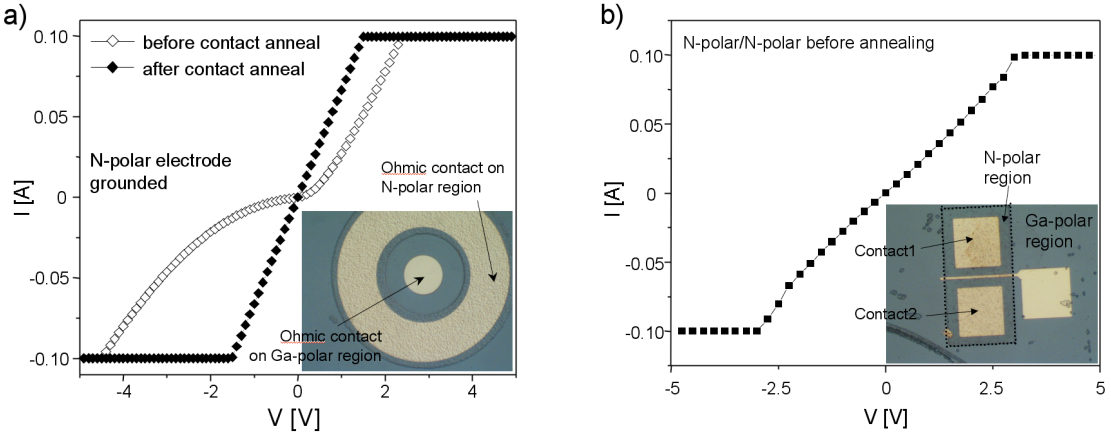

Figure 8. a) I-V characteristics of a N-polar/Ga-polar LPH with ohmic contacts prior and after annealing; b) I-V characteristics of ohmic contacts prior to the annealing on an N-polar region. The insets show optical micrographs of the measured structures. These measurements make it clear that any non-linearities prior to contact annealing are due to poor ohmic contacts on the Ga-polar region.

For this measurement, GaN films were grown with a total thickness of 2.0 μm. In the growth direction, the material comprised of 1.3 μm nominally undoped material, while the remaining 0.7 μm of the total thickness was intentionally doped with Si. Identically doped, large area Ga-polar films showed a carrier concentration of 6×10^{18} cm^{-3} and a mobility of μ_n=140 cm^2/Vs. By contrast, the electrical properties of intentionally Si-doped N-polar domains were not changed before and after doping, since even unintentionally N-polar domains showed significantly higher background carrier concentrations (> 10^{19} cm^{-3}). Ohmic contacts were fabricated both on N-polar and Ga-polar domains by e-beam evaporation and lift-off of Ti/Al/Ni/Au with thicknesses of 15 nm/200 nm/150 nm/105 nm, respectively. The *I-V* characteristic was recorded before and after the annealing of the contacts. The contact annealing was carried out in a N_2 atmosphere at 800°C for 35s. Figure 8(a) shows the *I-V* characteristics of a LPH prior and after the annealing of the contacts (the inset shows the optical micrograph of the

fabricated structure). Figure 8(b) shows the I-V characteristic measured between two contacts on a bar of N-polar material (see inset) prior to the contact anneal. The contacts on the N-polar domain showed linear characteristics without annealing due to the high doping concentration. Therefore, it is clear that the initially observed nonlinearity of the LPH was due to the non-ideal contacts on the Ga-polar side of the junction.

A linear current-voltage characteristic is obtained for the annealed contacts, suggesting that there is no potential barrier across the IDB. The characterization of the current transport across the IDB of a LPH and, moreover, across two IDBs is important for the possible application of LPHs to electronic devices in GaN. The discussed results suggest that for an *n*/*n* lateral polarity junction, there were no significant energy barriers for carrier transport at the IDB.

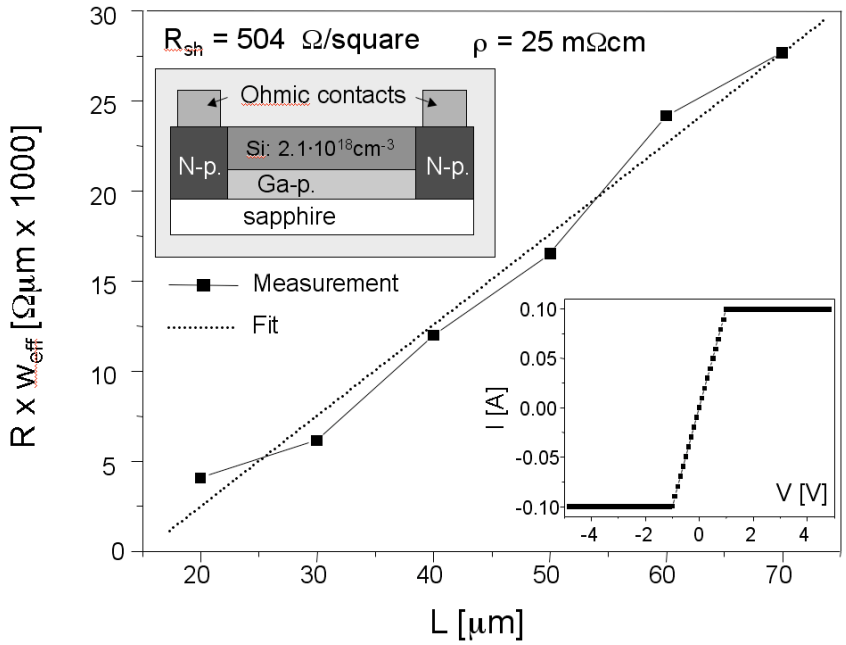

Figure 9. C-TLM measurement of the sheet resistance of the Ga-polar Si-doped layer with N-polar selectively doped ohmic contact regions. The upper inset shows the cross section of the measured double LPH structures, the lower inset shows the IV-characteristics of one N-polar/Ga-polar/N-polar double LPH structure. The values of the specific resistivity are in excellent agreement with values measured by Hall on Ga-polar layers grown with an identical dopant gas flux.

In addition to the above measurements, N-polar/Ga-polar/N-polar structures with two LPHs were characterized (see the lower inset in figure 9 for an I-V characteristic measured for a double LPH). The Ga-polar domain with its lower conductivity served as a channel sandwiched between the two heavily doped N-polar domains with Ohmic contacts on top (see upper inset in Figure 9). These structures were used to measure the sheet resistance and the resistivity of the Ga-polar films grown at identical growth conditions. The result of the circular transfer length method (C-TLM) measurement is shown in Figure 9. The measured resistance multiplied by the effective width of the circular structure was plotted against the distance as indicated by the linear fit line. The resistance of the N-polar domains can be neglected due to the higher conductivity (one

order of magnitude) and less than 10% contributed to the total length of the current path. The extracted sheet resistance was 504 Ω/sq and the resistivity was 25 mΩcm. These values were in good agreement with Hall measurements of Si-doped Ga-polar layers with similar carrier concentration. The discrepancy of these measurements was well within the reproducibility of the growth conditions. This further indicates that there was no influence of the LPH on the current transport across the IDB.

From the change of spontaneous polarization across the IDB, one would expect a polarization bound surface charge difference of 4×10^{13} electrons/cm^2, assuming that the spontaneous polarizations in the N-polar and Ga-polar regions are identical in magnitude and of opposite sign.[15] This would then lead to a significant potential difference across the IDB that would influence the carrier transport across the IDB even in the bulk of the LPH. However, as suggested by Rodriguez et al., over 99.9 % of the polarization bound surface charge is screened both in N-polar and Ga-polar GaN.[15] The total surface charge density difference across the IDB is below 4×10^{10} cm^{-2}. This number is insignificant with respect to the bulk charge concentration but for the lowest doping levels or channel carrier concentrations (doping levels below 10^{17} cm^{-3}).

6. Circular MESFET: Device Performance

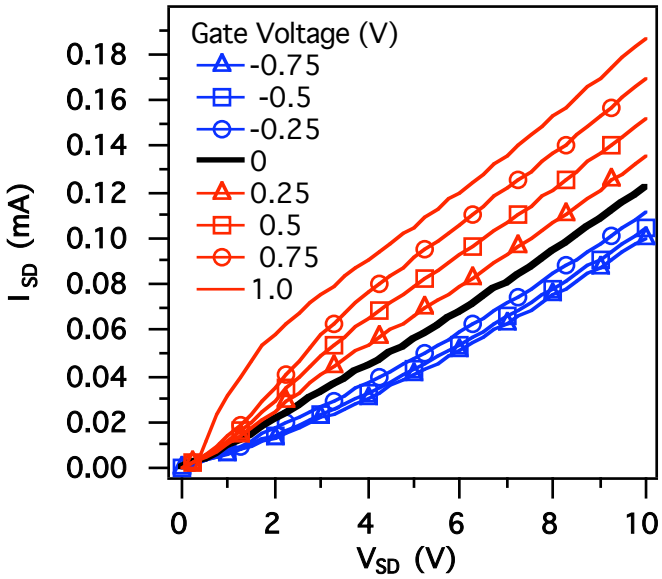

Figure 10. Source-drain current-voltage characteristic curves for the circular MESFET. Positive and negative gate voltages are depicted as red and blue lines, respectively. The expected pinch-off gate voltage for this configuration is –0.25 V.

Following the procedure described in section 2, circular MESFETs (Figure 4(a)) with N-polar domains as the source and drain contacts were fabricated. The gate width and length are 320 μm and 5 μm, respectively. No trench isolation was needed for this device design. The channel thickness is 30 nm with a cap of 30 nm of undoped GaN. Similar films with the same growth and SiH_4 dosage conditions as described in section 2 yielded an n-type carrier concentration of $3\text{x}10^{17}$ cm^{-3} with a mobility of 30 cm^2/Vs, as measured by the Hall effect. This would correspond to a channel sheet resistance of 230 kΩ/sq,

within the same order of magnitude as the sheet resistance from the 1.5 μm thick undoped GaN (figure 5(b)).

Figure 10 shows the source-drain current-voltage characteristic curves for this MESFET. Gate voltages were varied from 1.0 V to –0.75 V. The expected pinch-off gate voltage for this configuration and carrier concentration in the channel is –0.25 V. The maximum current attained at a 1 V gate voltage and 10 V as source-drain voltage was 0.18 mA or 0.56 mA/mm. Although some modulation of the gate above –0.25 V is observed, the nearly linear increase of the current with V_{SD} for gate voltage above and below pinch-off indicates that there is a parallel conduction path to the channel. This parallel conduction path seems to be the only path available for current conduction for gate voltages below pinch-off, within this applied gate voltage range it has not depleted that parasitic channel. Figure 11 shows the same characteristic curves but for gate voltages lower than –1 V. For smaller gate voltages (< -1 V), depletion is observed in the parasitic parallel channel.

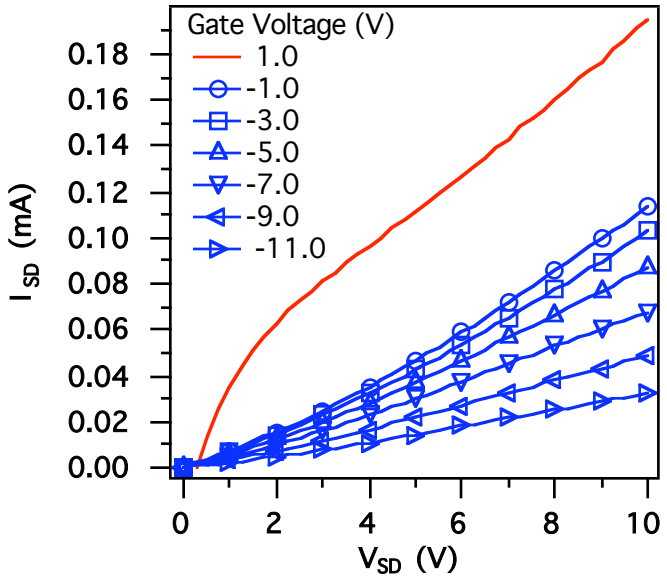

Figure 11. Source-drain current-voltage characteristic curves for the circular MESFET for gate voltages below –1 V.

The sheet resistances of the doped channel and the undoped GaN template are comparable, thus if the N-polar domains intended as the source and drain make an ohmic contact to the channel, they will also operate as ohmic contacts to the residual n-type carriers in the undoped GaN template (see figure 3) provided that ohmic contacts are possible given the low carrier concentration. Carrier mobility in the GaN template is expected to be less than 10 cm^2/Vs for the degree of compensation present, thus from the sheet resistance a carrier concentration of the order of $1x10^{15}$ cm^{-3} is expected. This is consistent with C-V measurements performed on Schottky diodes fabricated on Ga-polar GaN films (no LPH fabrication procedure) that indicated a net residual impurity concentration of $1x10^{15}$ cm^{-3}. Such a low carrier concentration in the template is necessary to observe depletion within the thickness of the undoped GaN template (pinch-off voltage < -3 V). The total charges in the channel and in the template are 0.14 μC cm^{-2}

(9 x 10^{11} cm^{-2}) and 0.03 μC cm^{-2} (2 x 10^{11} cm^{-2}), respectively. In future devices, this difference of only around 5 times needs to be increased by two orders of magnitude in order to obtain significant drain currents and transconductance. In this case, a low carrier concentration channel allowed us to probe the residual carrier concentration in the template and the quality of the ohmic contact of the N-polar domains as source and drain. Without these ohmic contacts, it would have been impossible to observe the parasitic parallel conduction channel.

7. Summary

In this exploratory research, we have identified key elements and demonstrated the feasibility of a LPH-based depletion-mode MESFET in which N-polar domains are used as lateral selectively doped areas to realize an ohmic contact to the n-channel. This was demonstrated by fabricating and operating an actual LPH-based MESFET. In addition, the electronic and structural properties of the two types of polar domains and the inversion domain boundary were studied to determine their role in the device structure.

The fabrication procedure consisted of patterning the LT-AlN nucleation layer and then growing the GaN structure with the desired channel doping and thickness. N-polar domains, with carrier concentration in the order of $1x10^{19}$ cm^{-3} were obtained where the LT-AlN film was removed. Insulating undoped Ga-polar domains were obtained on the regions with LT-AlN as the nucleation layer. The two domains were grown simultaneously with the selective doping as a property of the particular growth surface. Oxygen was found to be an impurity with up to three orders of magnitude higher concentration in N-polar domains than in the Ga-polar domains. In this way, the laterally doped selective areas were obtained without the need for other fabrication steps, like mass transfer or ion implantation. Certain processing steps, like additional ammonia anneals (nitridation) were necessary to achieve an LPH with higher sheet resistance of Ga-polar domains. These additional steps were necessary to recondition the LT-AlN nucleation layers after they were processed and patterned, in order to avoid the formation of inversion domains within the Ga-polar domains. Nevertheless, the role of the processing in introducing unwanted inversion domains needs to be clarified to improve on the insulating properties of the Ga-polar GaN and sharpness of the inversion domain boundary.

In addition to the LPH, the electronic properties of the inversion domain boundary (IDB) were studied. In order to use the N-polar domains as ohmic contacts to the channel, no electronic energy barrier that could form a depletion region across the boundary can exist. The designed structures were used to measure current-voltage curves for carrier transport across the boundary. No energy barrier was observed that would hinder the current transport for the doping levels used in the measurement, and the background carrier concentration observed in the undoped GaN template. The total surface charge density difference across the IDB was below 4×10^{10} cm^{-2} and insignificant with respect to the bulk charge concentration.

Current-voltage characteristics were measured for the LPH-based MESFET. They showed the existence of a parasitic parallel conduction channel with sheet resistance in the order of 1 MΩ/sq. This channel was observed due to the low carrier concentration in the actual conduction channel. This low carrier concentration in the channel prevented the device from reaching useful on-current levels. Nevertheless, the N-polar source-drain

contacts acted as excellent ohmic contacts to not only the device channel but also to the parasitic channel. Increasing the channel carrier concentration and mobility one order of magnitude by increasing the doping and changing the growth conditions will decrease the sheet resistance and increase the charge in the channel in order to reach useful current and transconductance levels.

---

[1] R. Collazo, S. Mita, A. Aleksov, R. Schlesser, and Z. Sitar, *J. Cryst. Growth,* **287**, 586 (2006).

[2] M. Stuzmann, O. Ambacher, M. Eickhoff, U. Karrer, A. Lima Pimenta, R. Neuberger, J. Schalwig, R. Dimitrov, P. J. Schuck, and R. D. Grober, *Phys. Stat. Sol. (b)* **228**, 505 (2001).

[3] R. Katayama, Y. Kuge, T. Kondo, and K. Onabe, *J. Cryst. Growth* **218**, 161 (2000).

[4] A. Chowdhury, H. M. Ng, M. Bhardwaj, and N. G. Weimann, *Appl. Phys. Lett*. **83**, 1077, (2003).

[5] F. A. Ponce, D. P. Bour, W. T. Young, M. Saunders, and J. W. Steeds, *Appl. Phys. Lett*. **69**, 337 (1996).

[6] M. Sumiya, M. Tanaka, K. Ohtsuka, S. Fuke, T. Ohnishi, I. Ohkubu, M. Yoshimoto, H. Koinuma, and M. Kawasaki, *Appl. Phys. Lett.* **75**, 674 (1999).

[7] R. Dalmau, R. Collazo, S. Mita, and Z. Sitar, *J. Electron. Mater.* **36**, 414 (2007).

[8] F. A. Ponce, D. P. Bour, W. T. Young, M. Saunders, and J. W. Steeds, *Appl. Phys. Lett*. **69**, 337 (1996).

[9] S. J. Pearton, F. Ren, A. P. Zhang, and K. P. Lee, *Mater. Sci. Eng., R*. **30**, 55 (2000).

[10] E. Frayssinet, W. Knap, P. Prystawko, M. Leszczynski, I. Grzegory, T. Suski, B. Beaumont, and P. Gibart, *J. Cryst. Growth* **218**, 161 (2000).

[11] T. K. Zywietz, J. Neugebauer, and M. Scheffler, *Appl. Phys. Lett*. **74**, 1695 (1999).

[12] M. Sumiya, K. Yoshimura, K. Ohtsuka, and S. Fuke, *Appl. Phys. Lett*. **76**, 2098, (2000).

[13] H. Heinke, V. Kirchner, S. Einfeldt, and D. Hommel, *Appl. Phys. Lett*. **77**, 2145 (2000).

[14] N. G. Weimann, L. F. Eastman, D. Doppalapudi, H. M. Ng, and T. D. Moustakas, *J. Appl. Phys*. **83**, 3656 (1998).

[15] B. J. Rodriguez, W. C. Yang, R. J. Nemanich, and A. Gruverman, *Appl. Phys. Lett.* **86**, 112115 (2005).